

TAOによる銀河形成研究 の新展開

筑波大学 計算科学研究センター

梅村 雅之

銀河形成の謎を解く

宇宙最初の星はいかなるものだったのか？ 最初の銀河はどのように生まれたのか？
巨大ブラックホールはなぜ存在するのか？

赤方偏移1000
(38万年)

宇宙の晴れ上がり

宇宙暗黒時代

初代星の誕生

原始ガスから生まれる星の質量は？

初代ブラックホールの誕生

巨大ブラックホールの種は何か？

赤方偏移10
(5億年)

宇宙再電離(宇宙の夜明け)

銀河形成時代

初代銀河の誕生

初代銀河はどのように生まれ、どのように再電離と関係したのか？

巨大ブラックホール形成

超臨界降着はあったか？

合体は起きたか？

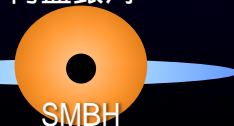


超巨大ブラックホール(SMBH) - 銀河バルジ関係

円盤銀河

楕円銀河

不規則銀河



銀河宇宙時代

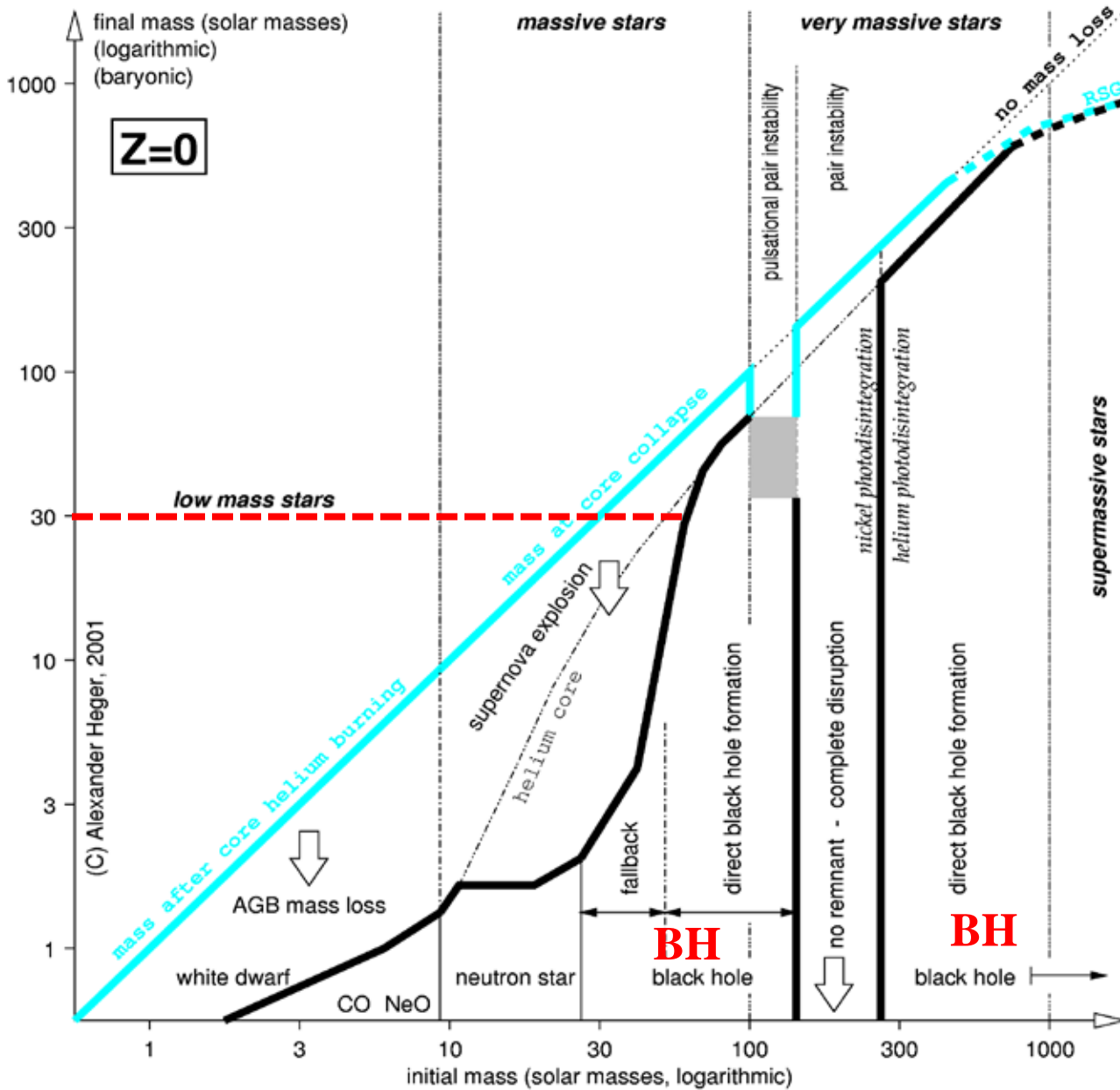
赤方偏移 0
(138億年)

なぜ銀河バルジ質量の1/1000なのか？

初代星の誕生

Pop III Star Evolution

Heger & Woosley 2002, ApJ, 567, 532



初代星の質量は？

a few $100M_{\odot}$

(Abel et al. 2000; Bromm et al. 2002; Yoshida et al. 2006)

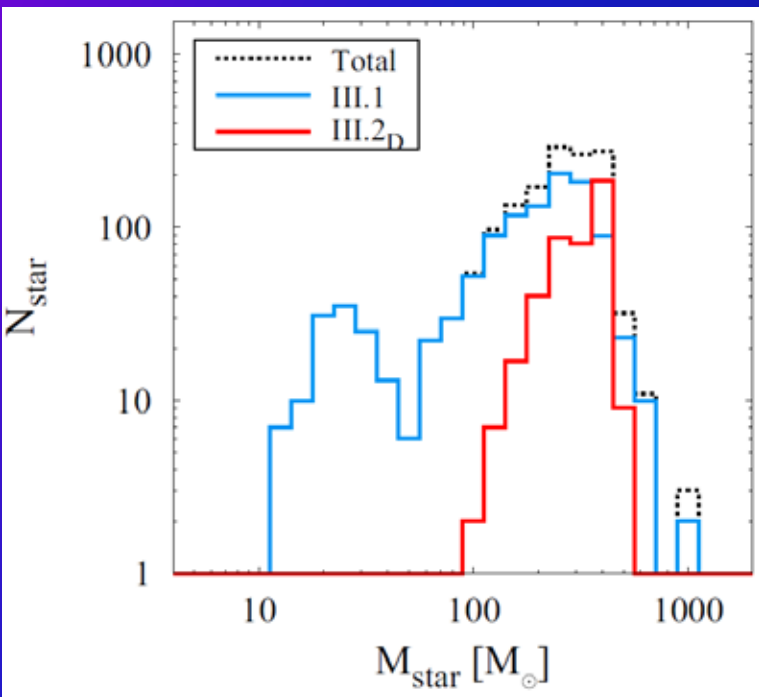
bimodal of $\sim 1M_{\odot}$ & a few $100M_{\odot}$ (Nakamura & Umemura 2001)

several $10M_{\odot}$ (Clark et al. 2011)

about $40M_{\odot}$ (Hosokawa et al. 2011)

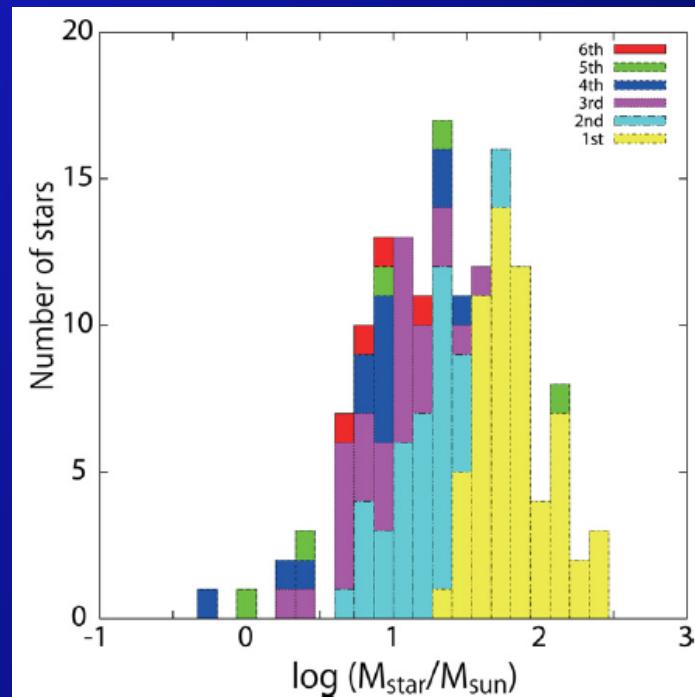
a few $\sim 10M_{\odot}$ (Greif et al. 2011)

Runaway

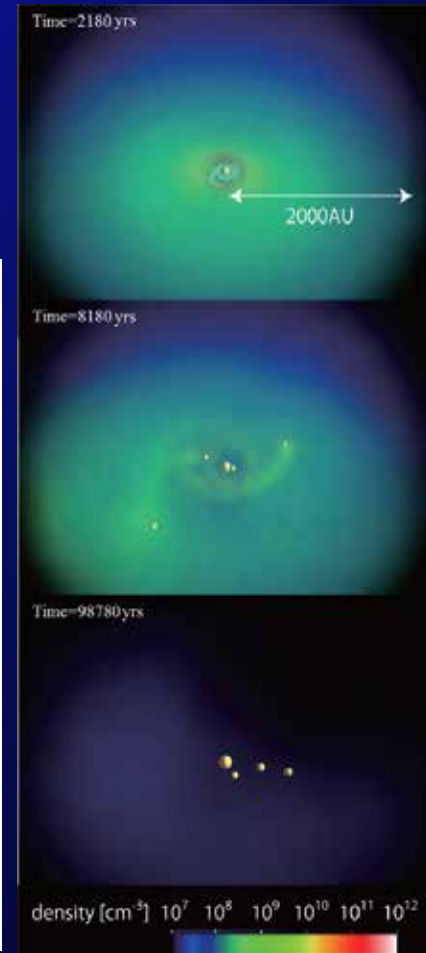


Hirano et al. MNRAS 448, 568 (2015)

Accretion

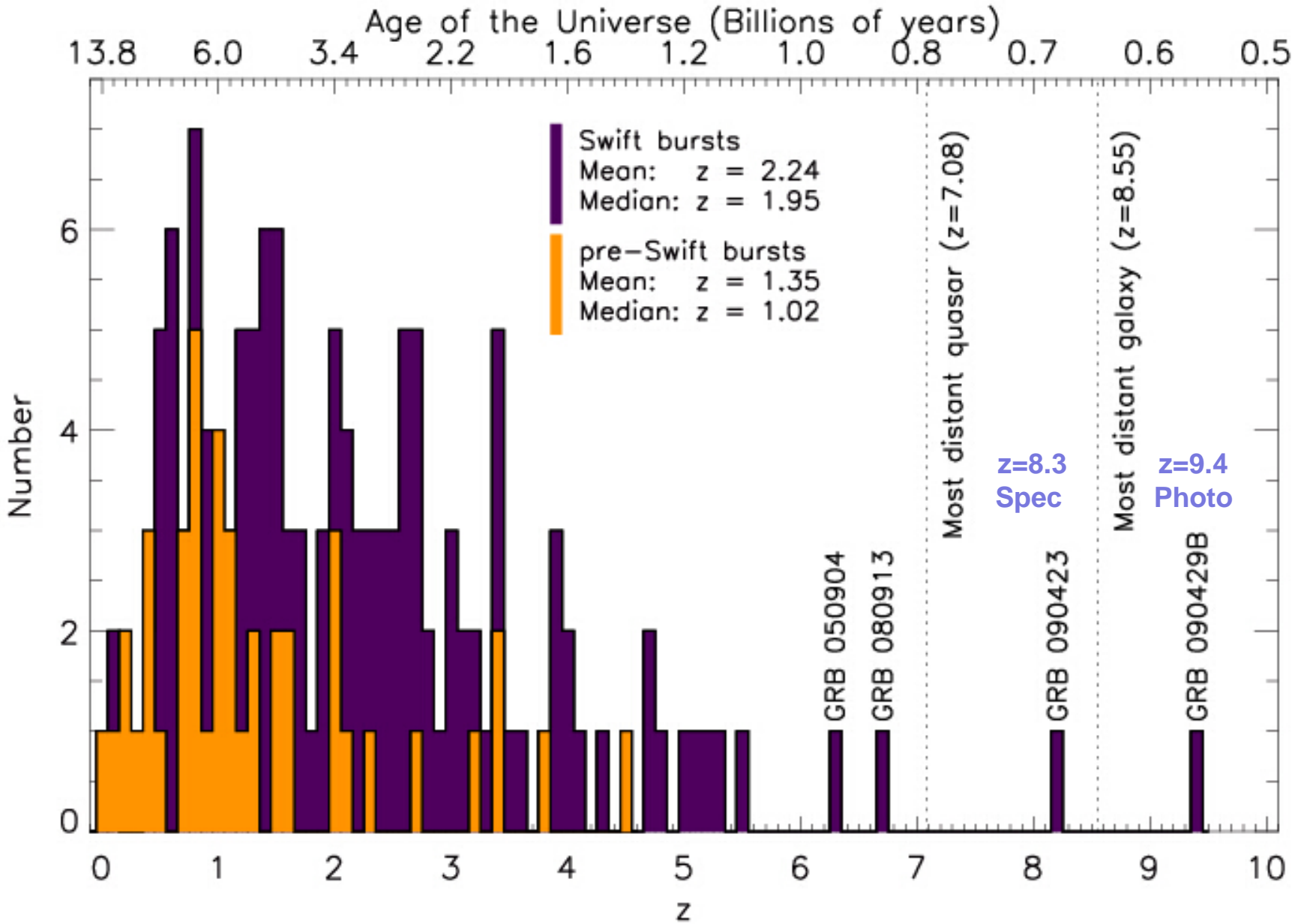


Susa, et al. ApJ, 792, 32 (2014)



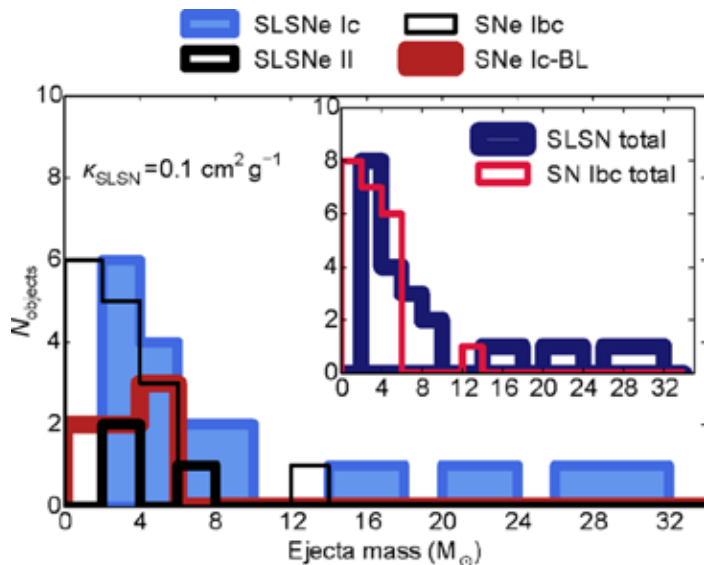
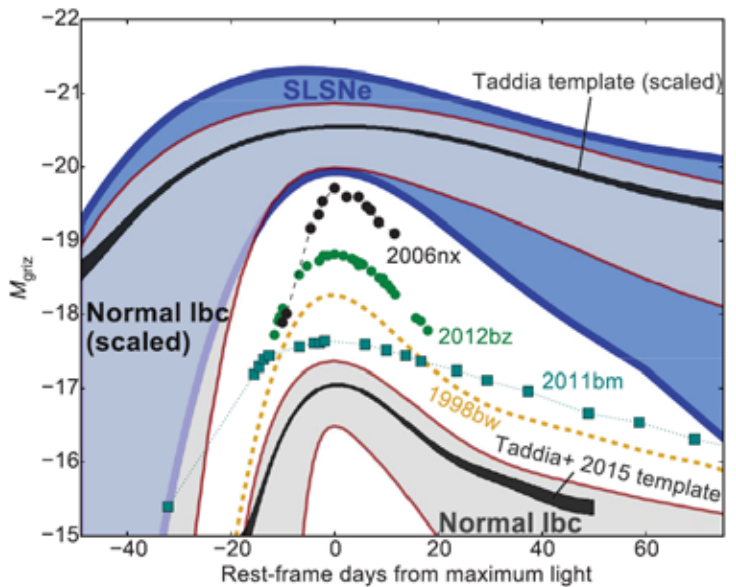
GRB赤方偏移分布

$z=11.1$
galaxy
↓

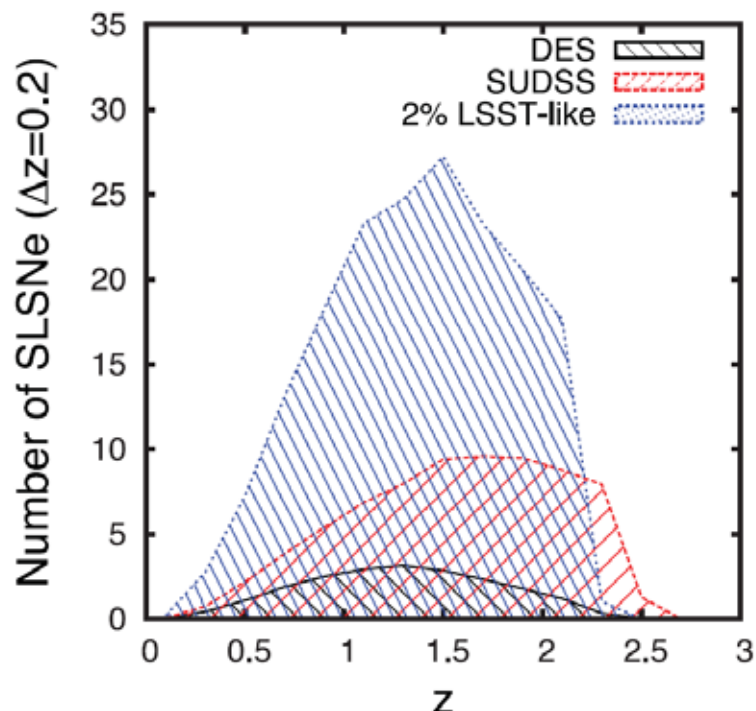


SLSNe: Superluminous Supernovae

Nicholl et al. MNRAS **452**, 3869–3893 (2015)

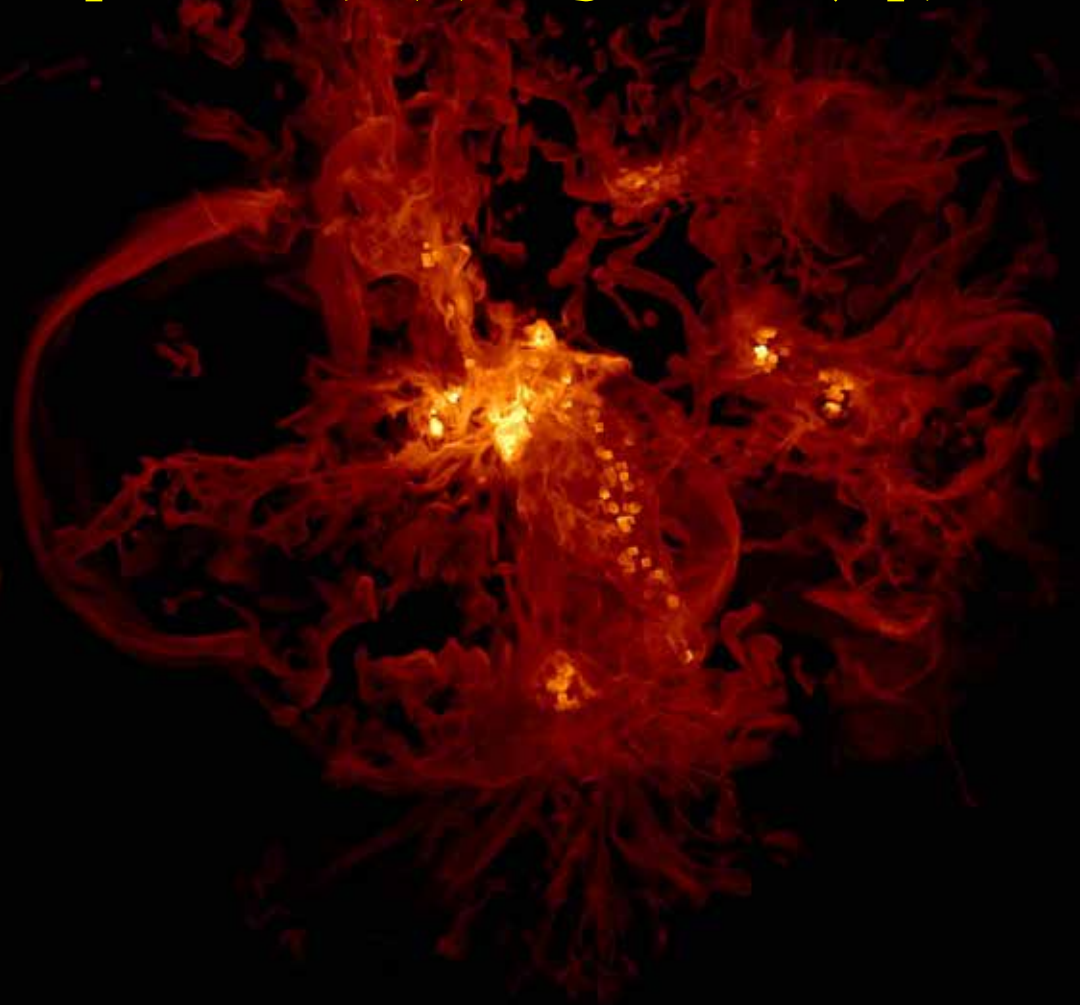


- $m > 50 M_{\odot}$ の星の爆発 (PISNの可能性も?)
- これまで $z < 2.5$ で観測
- TAOによる赤外観測



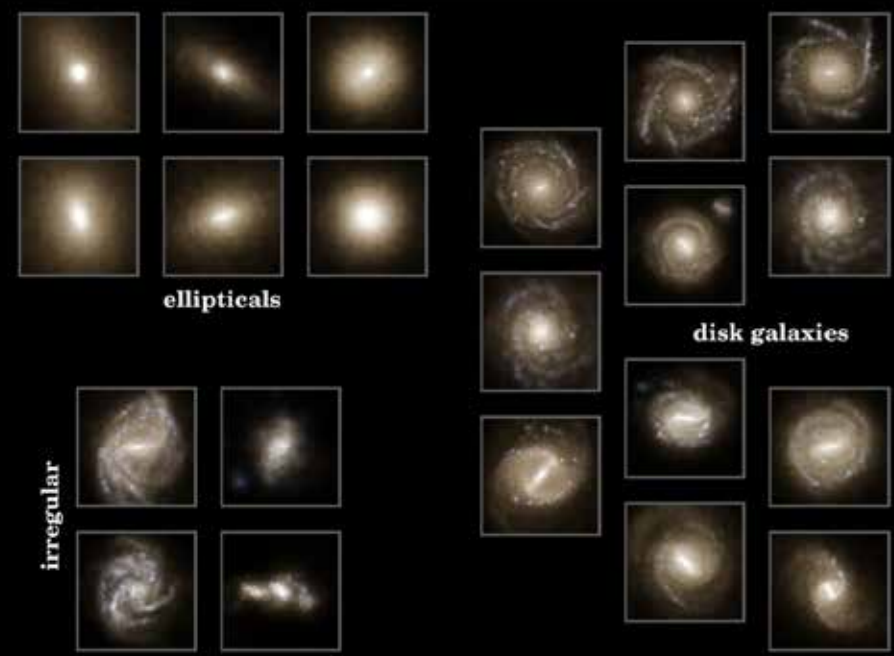
Scovacricchi et al. MNRAS **456**, 1700–1707 (2016)

初代銀河の形成



The Illustris Simulation

M. Vogelsberger · S. Genel · V. Springel · P. Torrey · D. Sijacki · D. Xu · G. Snyder · S. Bird · D. Nelson · L. Hernquist



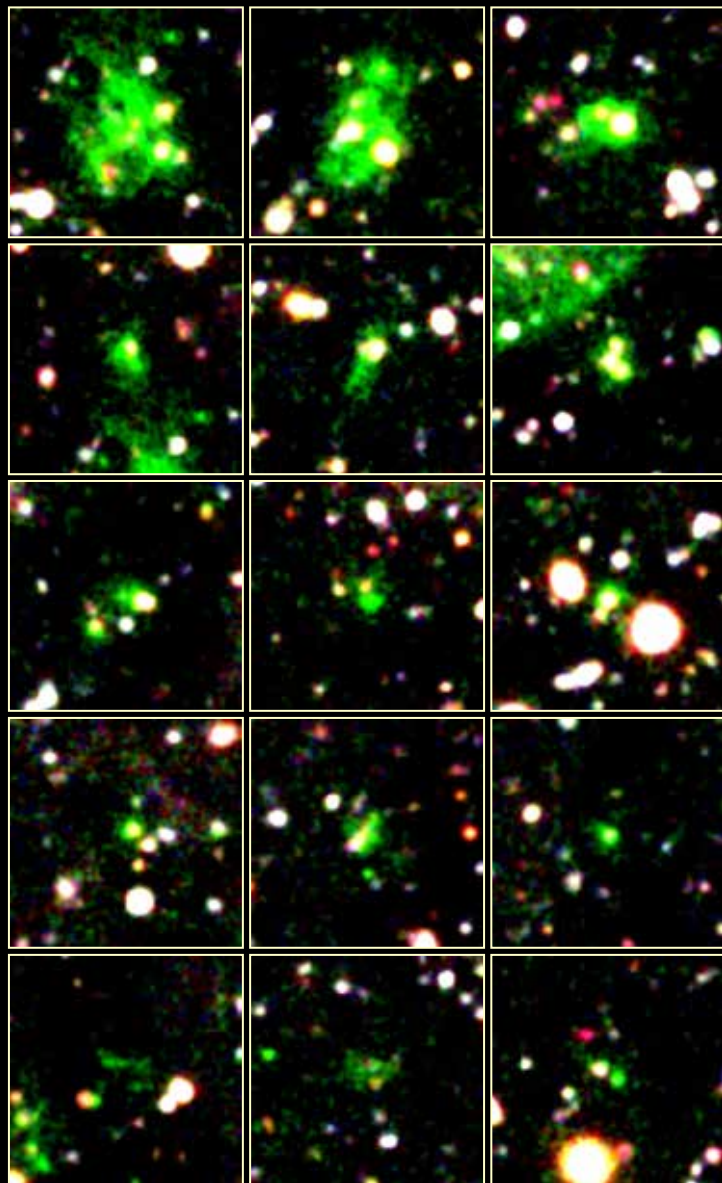
Vogelsberger et al. 2014,
nature, 509, 177

ライマン α 輝線天体(LAE)

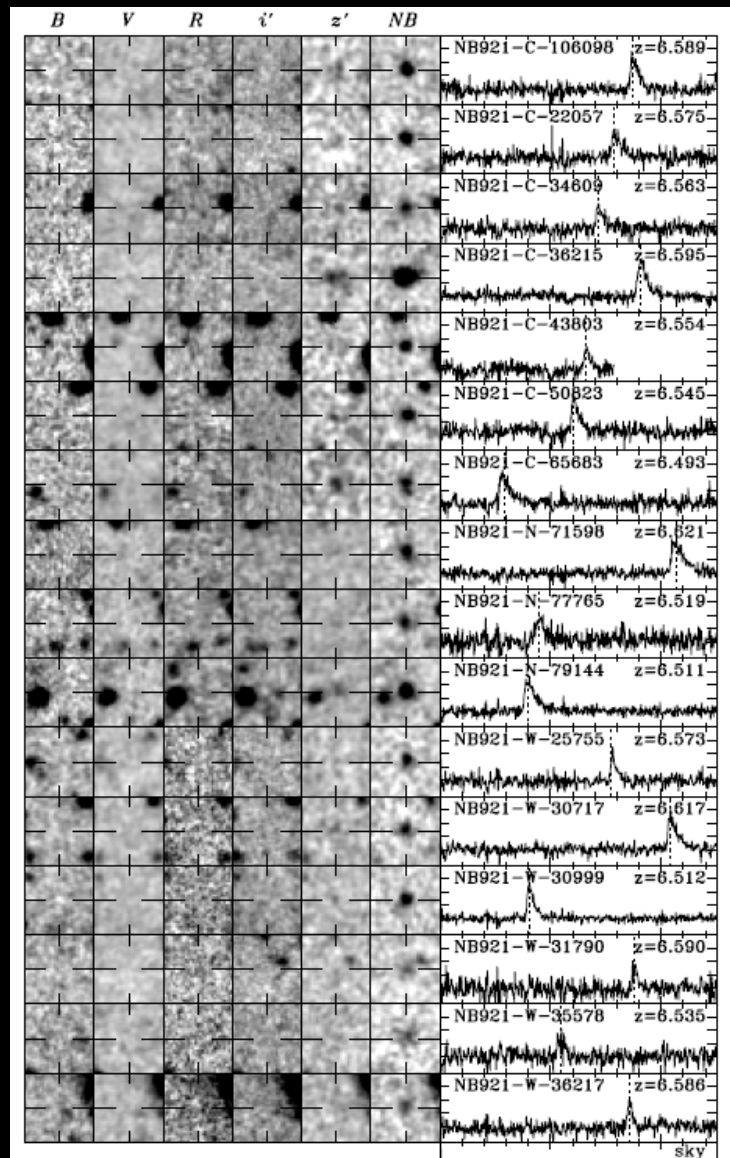
$z \sim 3$

$L=10^8-10^{10}L_e$

$z \sim 7$



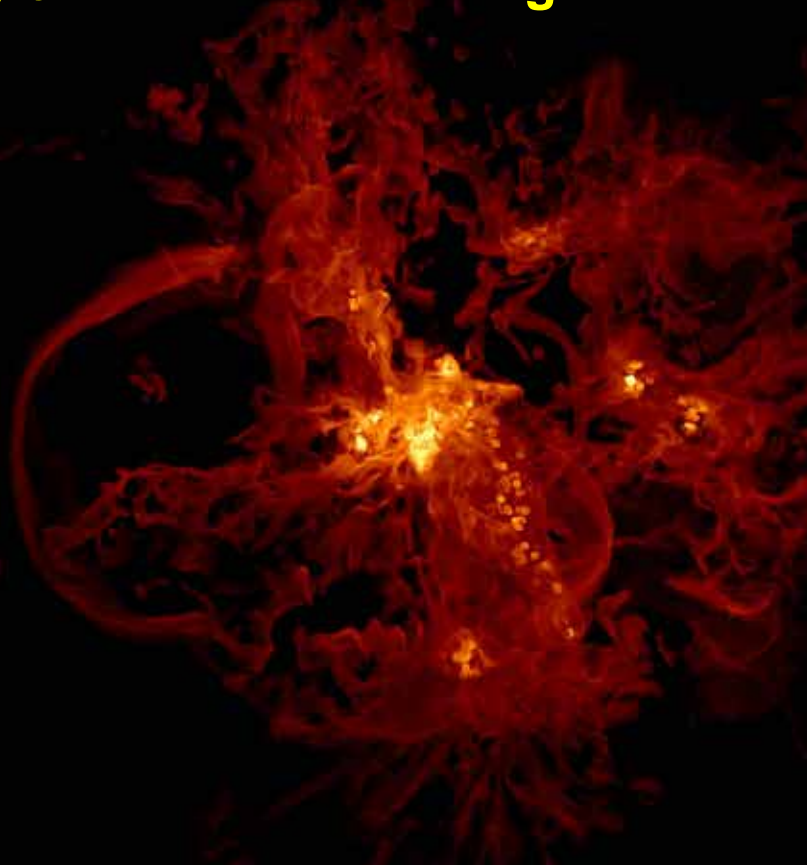
Matsuda et al 2004, ApJ, 128, 569



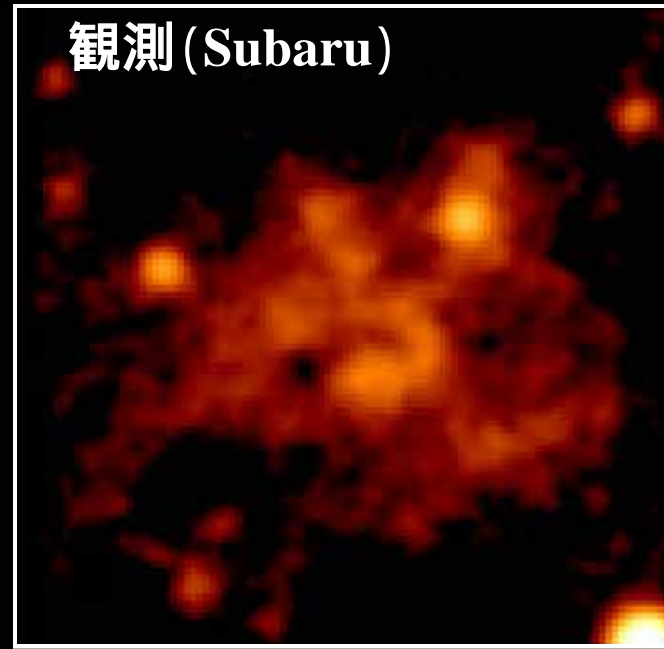
Ouchi et al. 2010, ApJ, 723, 869

超新星爆発モデル

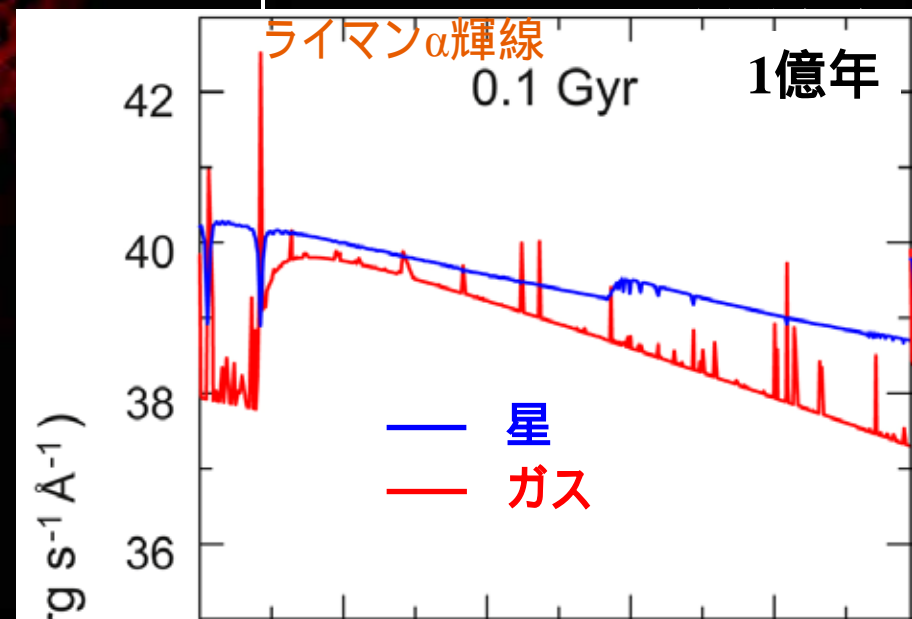
Ly α emission = cooling shells



観測 (Subaru)



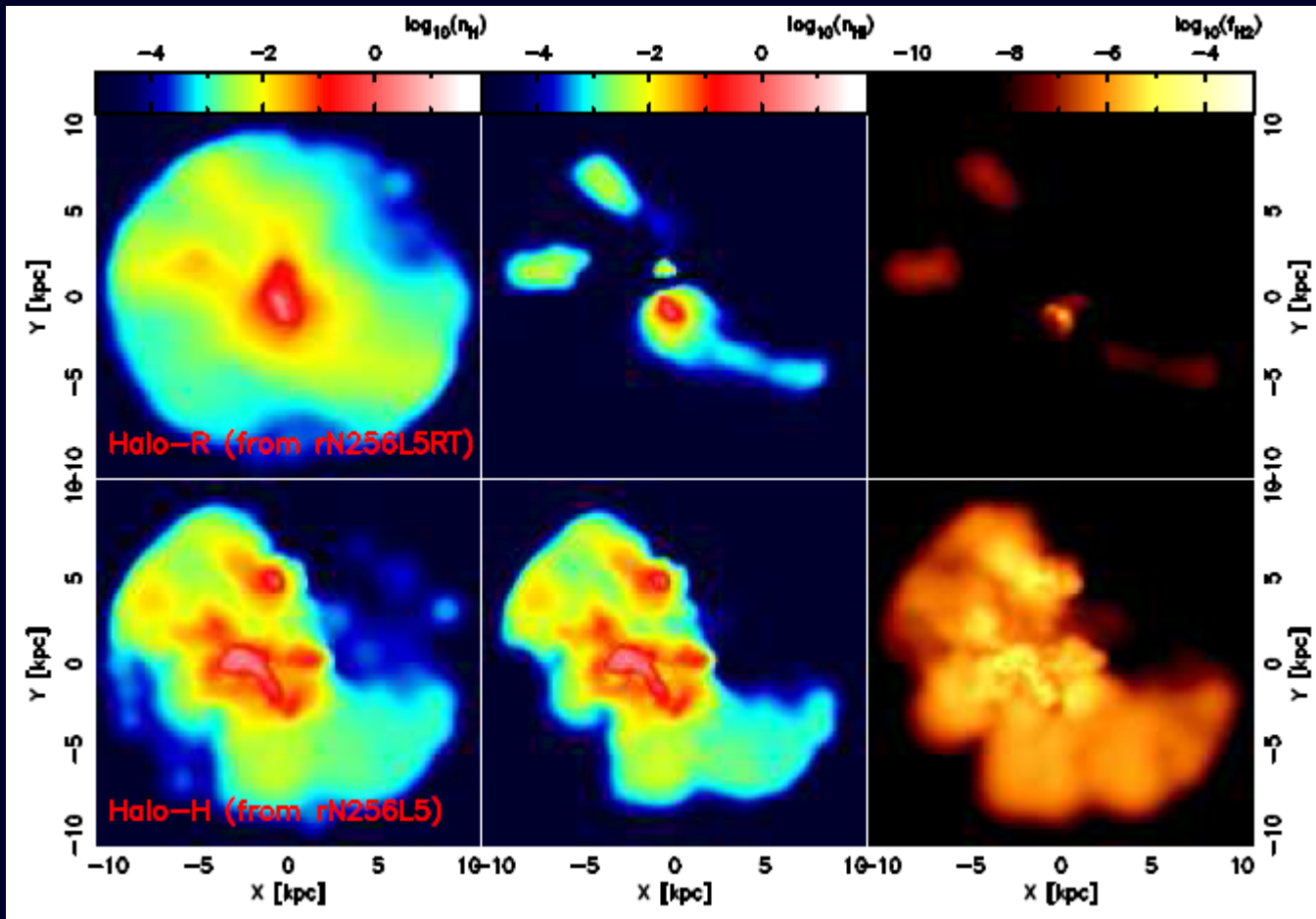
Mori and Umemura, 2006,
Nature, 440, 644



光電離モデル

光電離モデル+SN (内部 & 外部電離輻射)

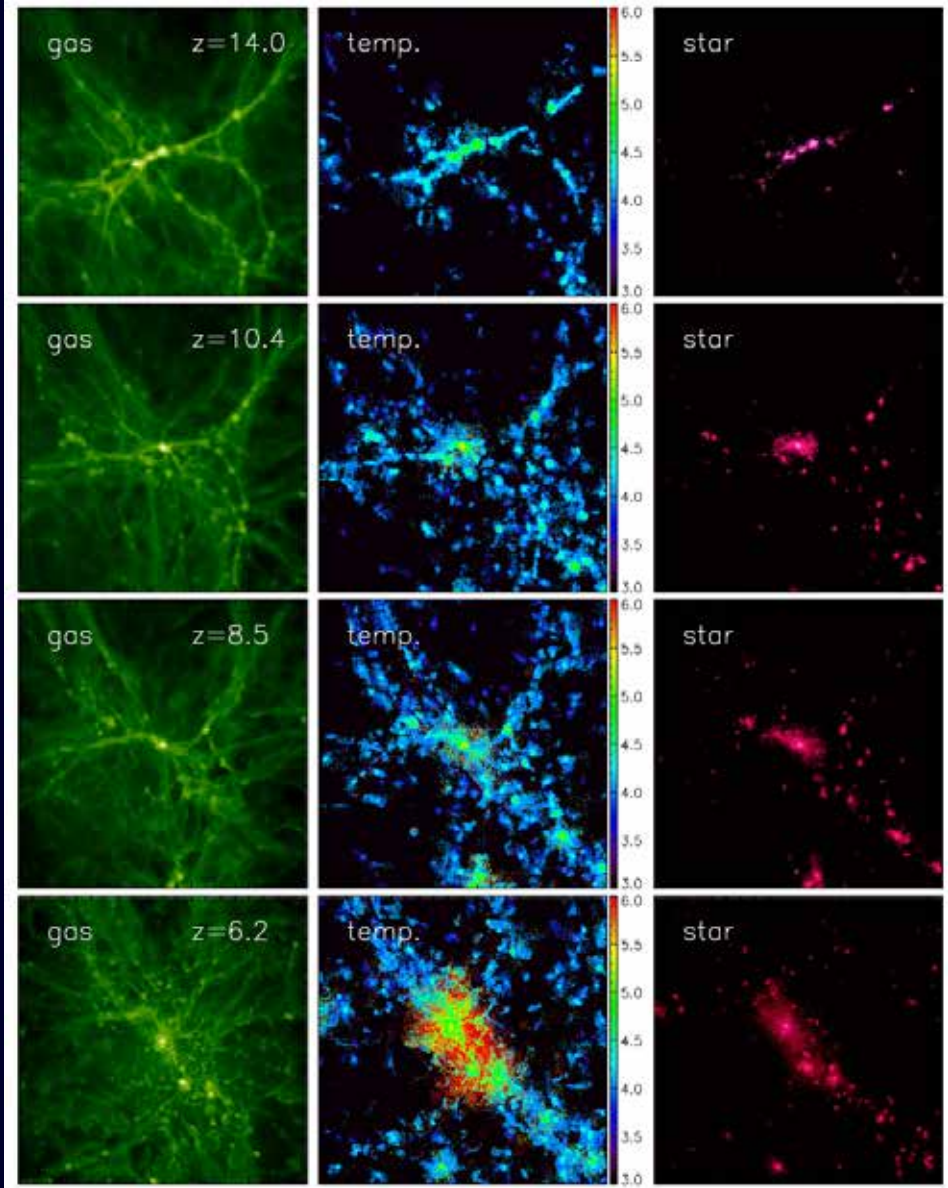
Ly α emission = recombination in HII regions



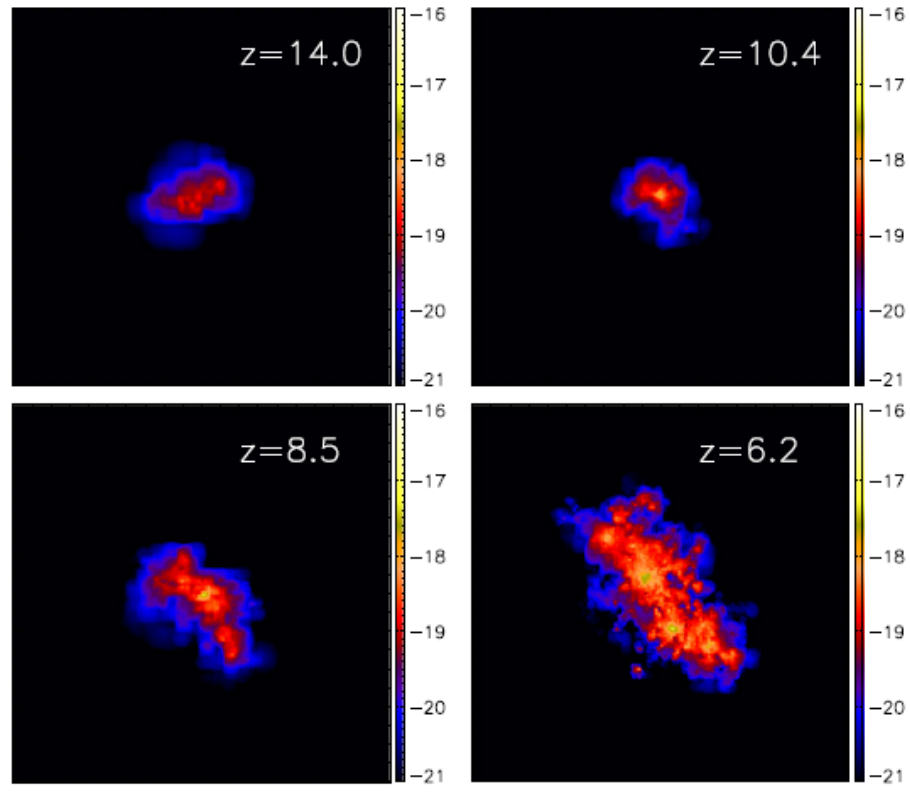
Hasegawa & Semelin 2012, MNRAS, 428, 154

MU, Susa, Hasegawa, Suwa & Semelin 2012, PTEP, 01A306 (23pp)

Cold Accretion モデル



Ly α emission = cooling radiation



Yajima et al 2015, 801, 52

HeII detection in CR7

Sobral et al. 2015, ApJ, 808, 139

COSMOS/Ultra VISTA Fields

VLT (X-SHOOTER, SINFONI, FORS2), Keck (DEMIOS)

CR7 : $z=6.604$ ($L_{\text{Ly}\alpha}=8.5 \cdot 10^{43}$ erg/s)

cf. Himiko: $z=6.54$ ($L_{\text{Ly}\alpha}=2.5 \cdot 10^{43}$ erg/s)

J-band excess 6s detection of HeII 1640 Å (S/N=6)

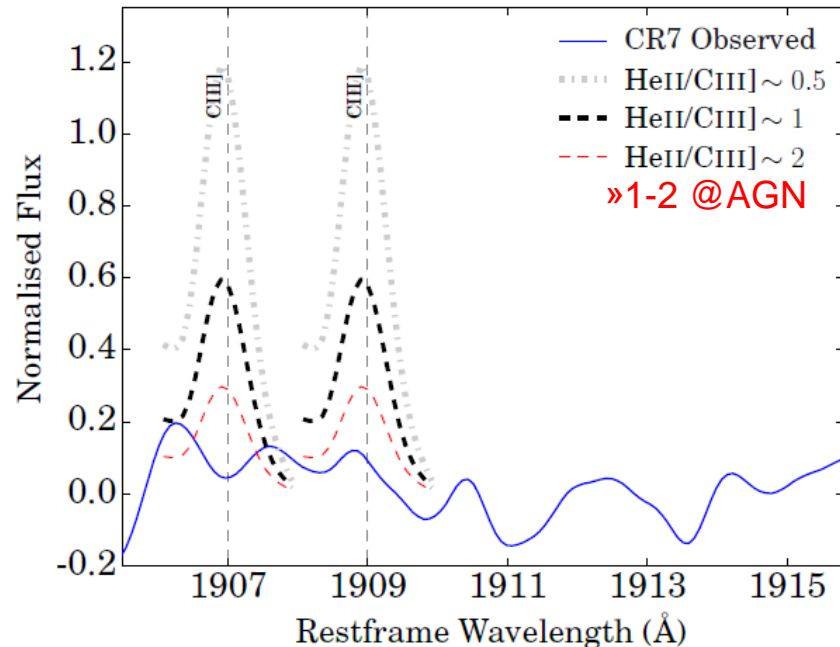
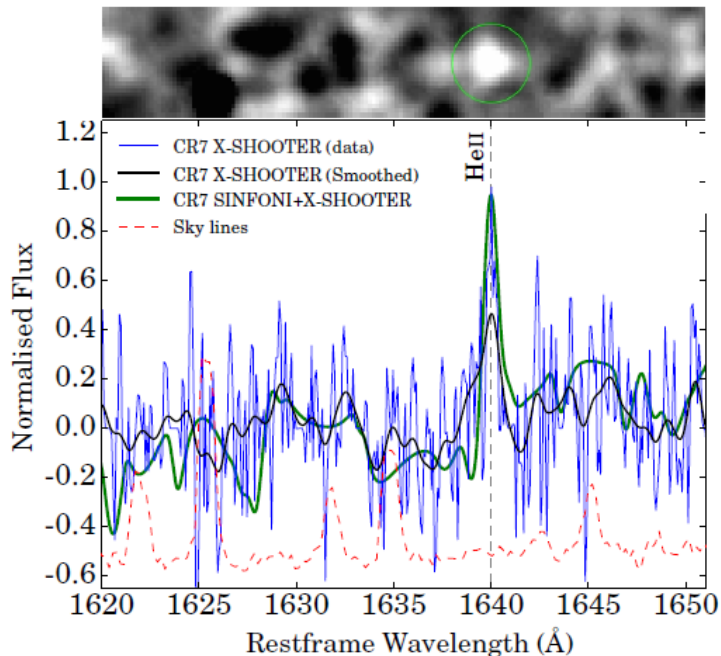
$F_{\text{HeII}}=4.1 \cdot 10^{-17}$ erg/s/cm²

FWHM=130 ± 30 km/s

HeII/Lyα=0.23

NV/Lyα < 1/70, CIII]/HeII < 0.4 (weak metal line emission)

NV1240, NIV1487, CIV1549, OIII]1661, OIII]1666, NIII]1750: undetected



CR7は何者か

Possible sources for high luminosity, high EW Ly a and HeII

1) Cooling radiation (Faucher-Giguère et al. 2010)

R $L_{\text{Ly}\alpha} = 10^{44}$ erg/s @ $M_{\text{halo}} > 5 \times 10^{11} M_{\odot}$

R expected number density $\sim 10^{-5} \text{Mpc}^{-3}$ @ $z \sim 6.6$ consistent with obs.

HeII/Ly α < 0.1

broader Ly α line

2) Strong AGN (De Breuck et al. 2000)

HeII FWHM ~ 1000 km/s

strong metal lines (NV, OIII], CIII])

3) Wolf-Rayet (WR) stars (Shirazi & Brinchmann 2012; Erb et al. 2010)

line FWHM ~ 3000 km/s

many metal lines

4) Direct collapse black hole (Johnson et al. 2011)

R high HeII/Ly α

R no metal line

strong X-ray emission

broad line emission

much lower Ly α & HeII luminosities

5) PopIII stars (Schaerer 2003; Raiter et al. 2010)

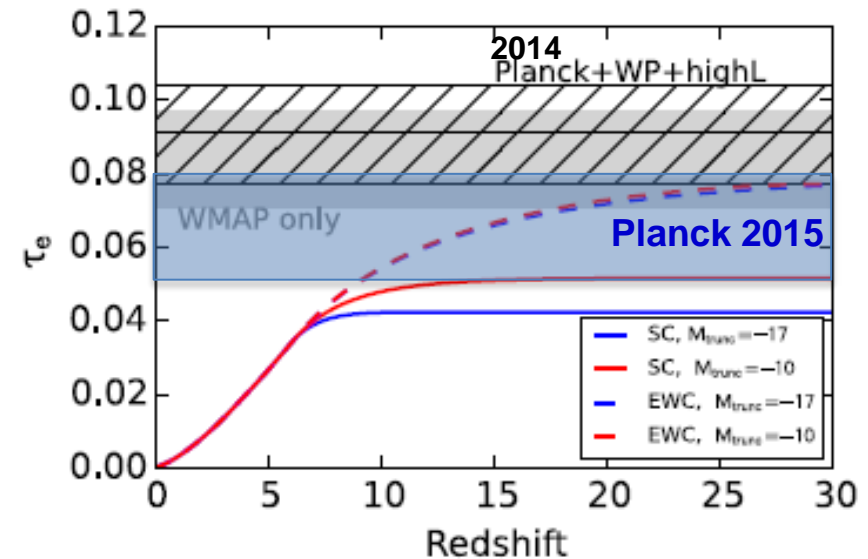
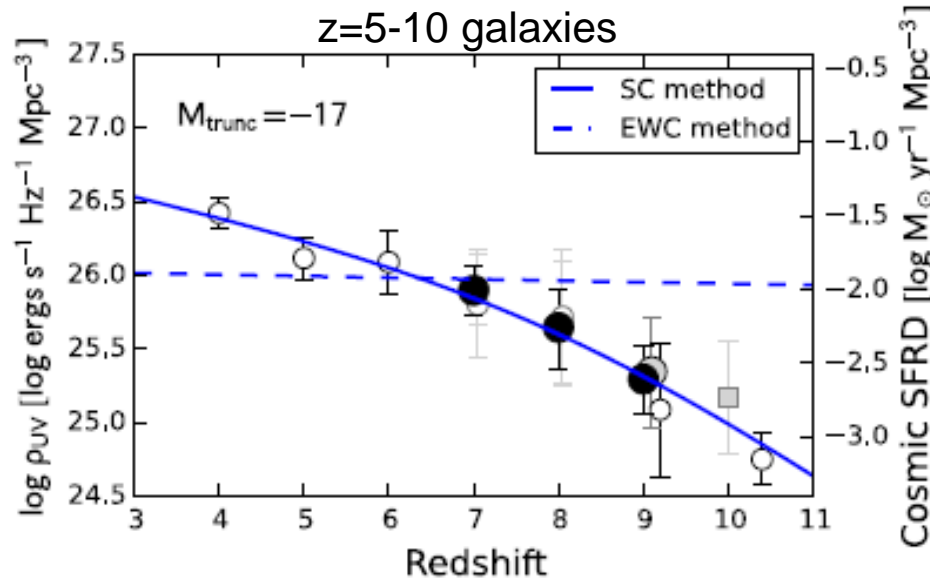
R HeII FWHM ~ 100 km/s

R HeII/Ly α ~ 0.1 @ HeII/Ly α $\sim 0.2-0.3$ due to HI absorption

R no metal line

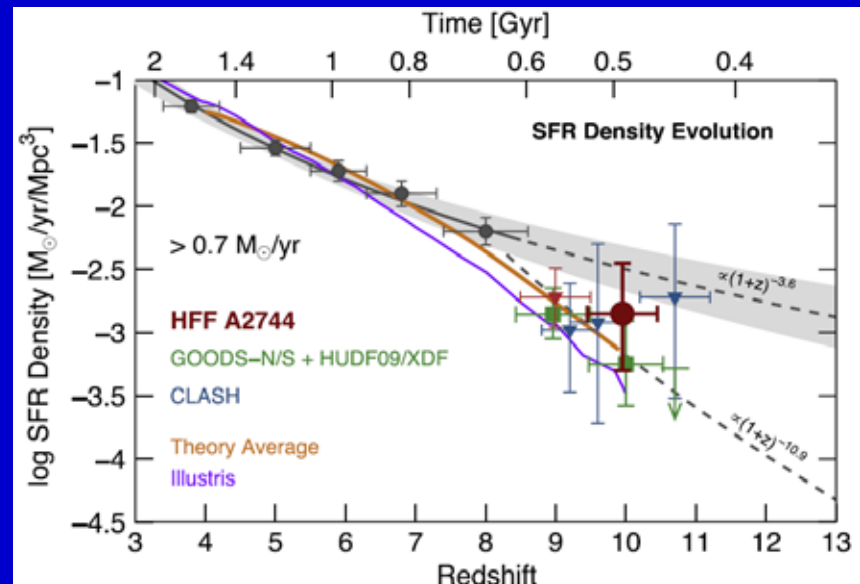
原始銀河の光度関数と宇宙再電離

Ishigaki et al, 2015, ApJ, 799,12



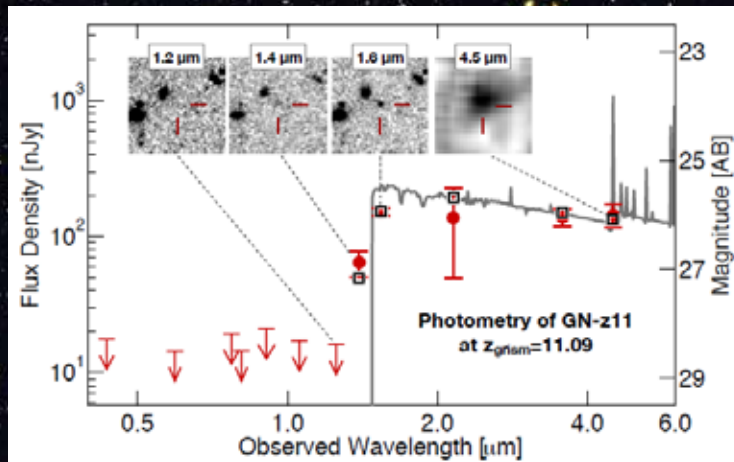
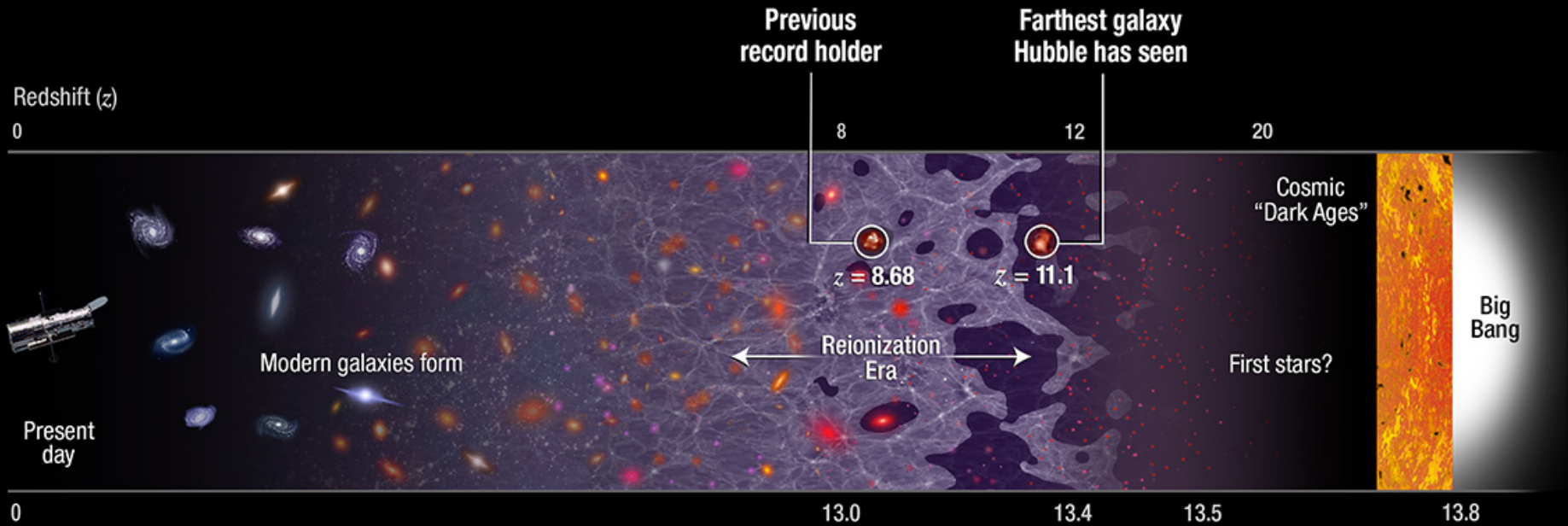
Cosmic Star Formation Rate
Density at $z \sim 10$

Oesch et al. 2015, ApJ, 808,104

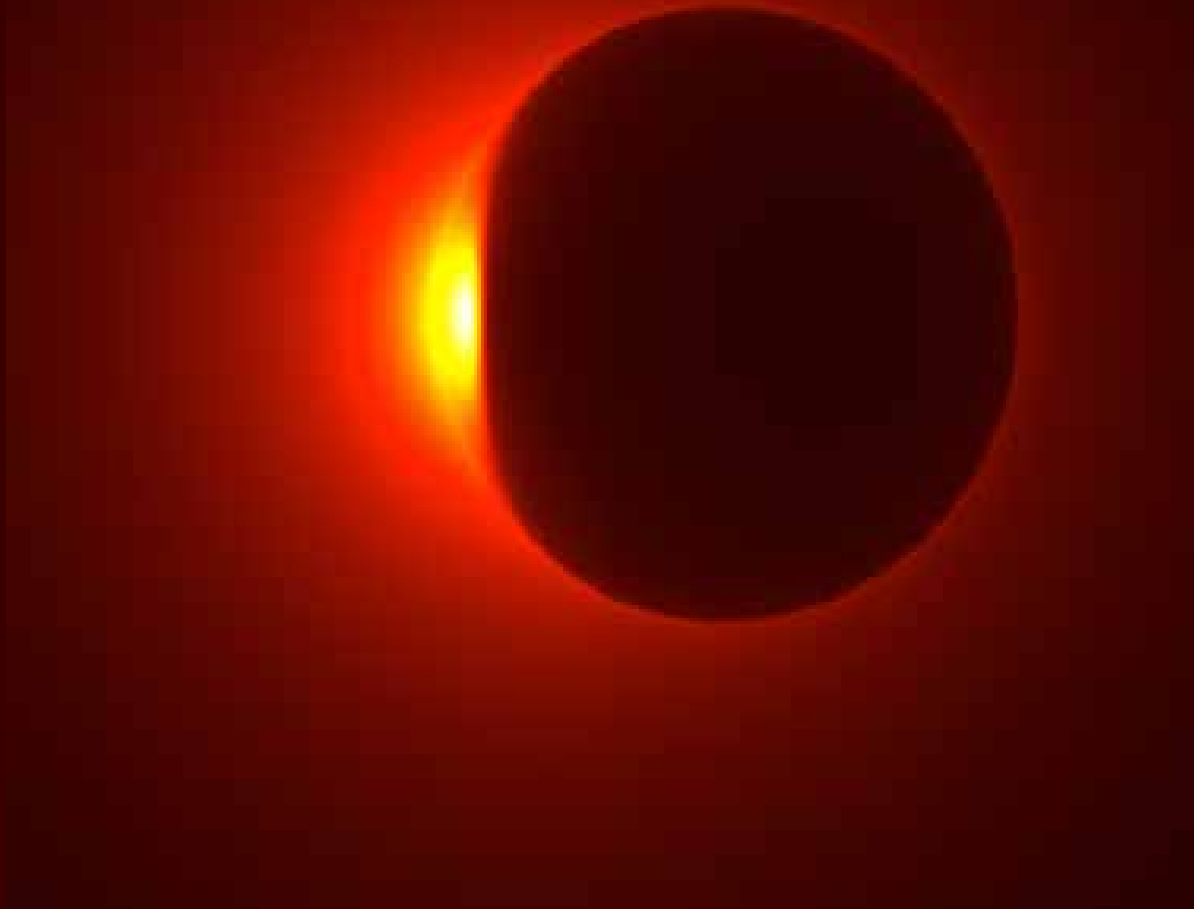


$z=11.1$ 銀河の発見

Oesch et al. 2016, arXiv:1603.00461



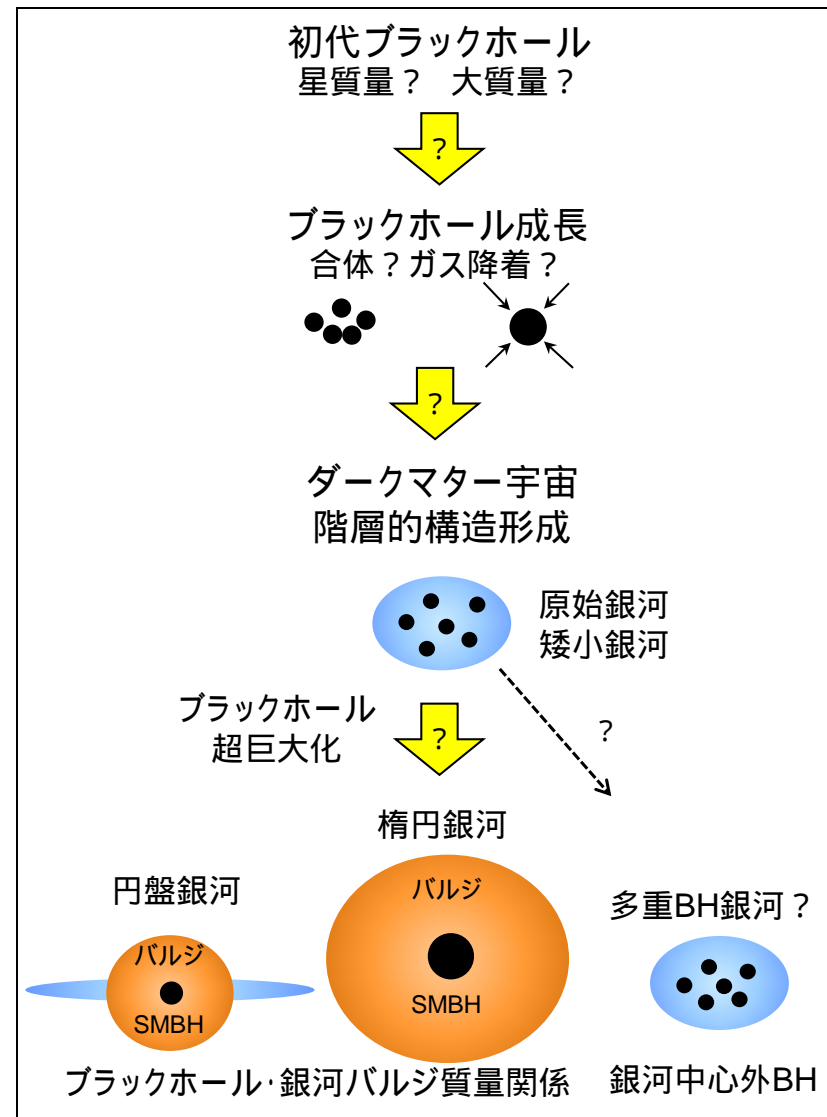
巨大ブラックホールの起源



超巨大ブラックホール起源：7つの疑問

2020年代を見据えて

- Q1: 初代ブラックホールは星質量(数 $\sim 10M_{\odot}$)だったのか大質量(数万 \sim 数10万 M_{\odot})だったのか
- Q2: Building block はどこにあるのか(宇宙論的SMBH形成)
- Q3: SMBHは質量降着で成長したのか合体で成長したのか
- Q4: SMBHはなぜ銀河バルジ質量の1000分の1になっているのか
- Q5: SMBHは銀河中心にしかできないのか
- Q6: SMBHの"ダウンサイジング"は何を意味しているのか
- Q7: 矮小楕円銀河にはなぜSMBHはないのか



z=7.085 QSO

Mortlock et al. 2011, nature, 474, 616

$$L = 6.3 \times 10^{13} L_{\alpha}, \quad M_{\text{BH}} = 2 \times 10^9 M_{\alpha}$$

Eddington Ratio $n_E = 1.2$ (Super-Eddington Accretion)

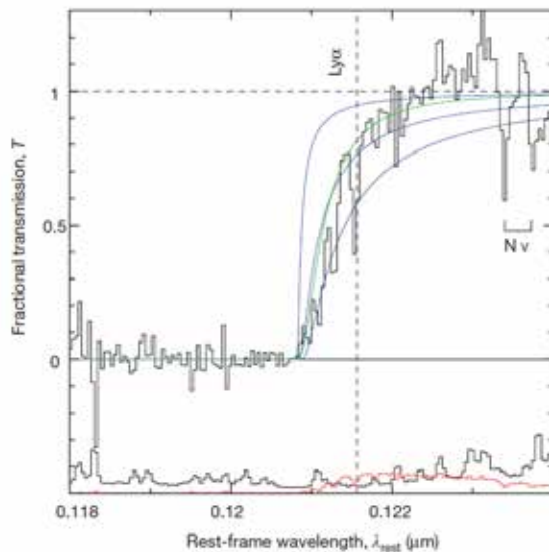
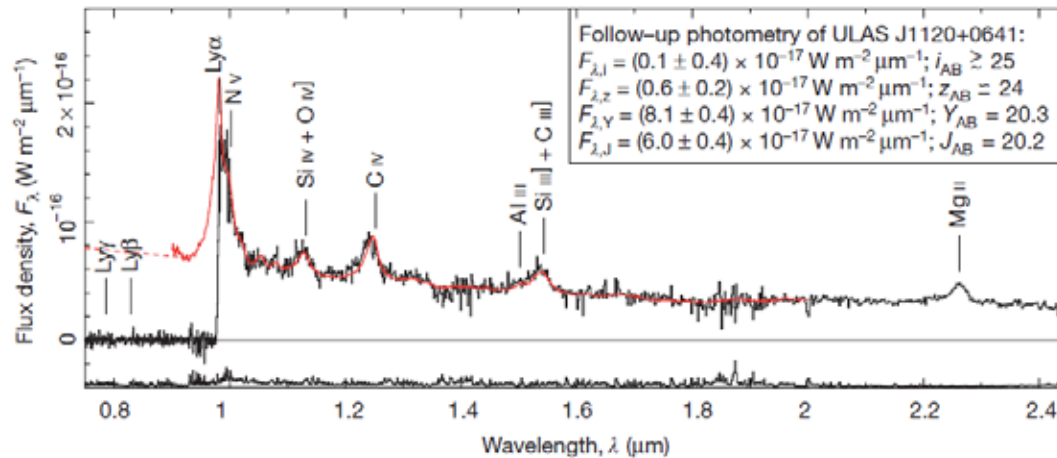


Figure 4 | Rest-frame transmission profile of ULAS J1120+0641 in the region of the Ly α emission line, compared to several damping profiles. The transmission profile of ULAS J1120+0641, obtained by dividing the spectrum by the SDSS composite shown in Fig. 1, is shown in black. The random error spectrum is plotted below the data, also in black. The positive residuals near 0.1230 μm in the transmission profile suggest that the Ly α emission line of ULAS J1120+0641 is actually stronger than average, in which case the absorption would be greater than illustrated. The dispersion in the Ly α equivalent width at a fixed C IV equivalent width of 13% quantifies the uncertainty in the Ly α strength; this systematic uncertainty in the transmission profile is shown in red. The blue curves show the Ly α damping wing of the intergalactic medium for neutral fractions of (from top to bottom) $f_{\text{HI}} = 0.1$, $f_{\text{HI}} = 0.5$ and $f_{\text{HI}} = 1.0$, assuming a sharp ionization front 2.2 Mpc in front of the quasar. The green curve shows the absorption profile of a damped Ly α absorber of column density $N_{\text{HI}} = 4 \times 10^{20} \text{ cm}^{-2}$ located 2.6 Mpc in front of the quasar. These curves assume that the ionized zone itself is completely transparent; a more realistic model of the H I distribution around the quasar might be sufficient to discriminate between these two models^{25,27}. The wavelength of the Ly α transition is shown as a dashed line; also marked is the N V doublet of the associated absorber referred to in the text.

$$L=4.29' 10^{14}L_{\alpha}, \quad M_{\text{BH}}=1.2' 10^{10}M_{\alpha}$$

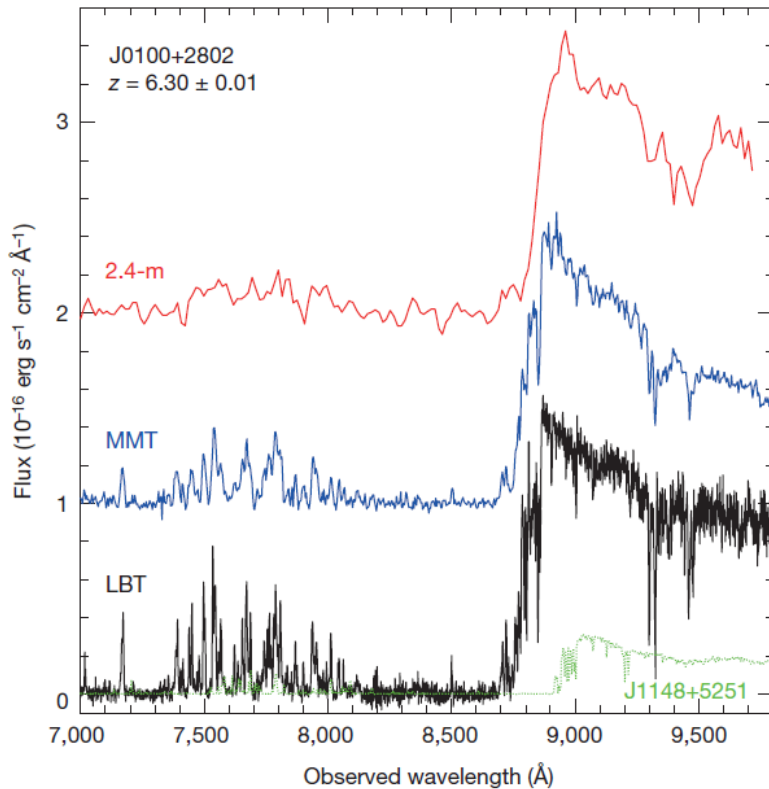


Figure 1 | The optical spectra of J0100+2802. From top to bottom, spectra taken with the Lijiang 2.4-m telescope, the MMT and the LBT (in red, blue and black colours), respectively. For clarity, two spectra are offset upward by one and two vertical units. Although the spectral resolution varies from very low to medium, in all spectra the Ly α emission line, with a rest-frame wavelength of 1,216 \AA , is redshifted to around 8,900 \AA , giving a redshift of 6.30. J0100+2802 is a weak-line quasar with continuum luminosity about four times higher than that of SDSS J1148+5251 (in green on the same flux scale)¹, which was previously the most luminous high-redshift quasar known at $z = 6.42$.

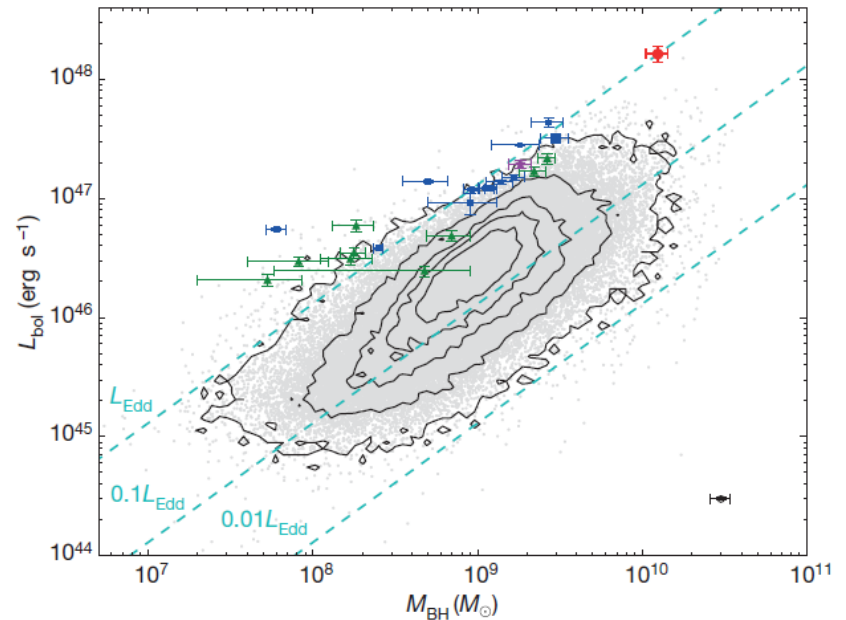


Figure 4 | Distribution of quasar bolometric luminosities, L_{bol} , and black-hole masses, M_{BH} , estimated from the Mg II lines. The red circle at top right represents J0100+2802. The small blue squares denote SDSS high-redshift quasars^{2,10,12}, and the large blue square represents J1148+5251. The green triangles denote CFHQS high-redshift quasars^{11,12}. The purple star denotes ULAS J1120+0641 at $z = 7.085$ (ref. 6). Black contours (which indicate 1 σ to 5 σ significance from inner to outer) and grey dots denote SDSS low-redshift quasars²¹ (with broad absorption line quasars excluded). Error bars represent the 1 σ standard deviation, and the mean error bar for low-redshift quasars is presented in the bottom-right corner. The dashed lines denote the luminosity in different fractions of the Eddington luminosity, L_{Edd} . Note that the black-hole mass and bolometric luminosity are calculated using the same method and the same cosmology model as in the present Letter, and the systematic uncertainties (not included in the error bars) of virial black-hole masses could be up to a factor of three²⁷.

Eddington Growth of z=7.085 QSO SMBH

$$M_{\text{BH}}(t) = M_0 \exp\left(\frac{t}{t_E} n_E\right), \quad t_E \approx \frac{M}{\dot{M}_E} = 4.5 \cdot 10^7 \frac{M}{0.1 M_\odot} \text{ yr}$$

$$z_{\text{PopIII}} = 20 \quad (t = 1.83 \cdot 10^8 \text{ yr}), \quad M_0 = 30 M_\odot$$

$$z_{\text{QSO}} = 7.085 \quad (t = 7.83 \cdot 10^8 \text{ yr}), \quad M_{\text{BH}} = 2 \cdot 10^9 M_\odot$$



$$\text{Eddington ratio } n_E = 1.4$$

Eddington Growth of z=6.30 QSO SMBH

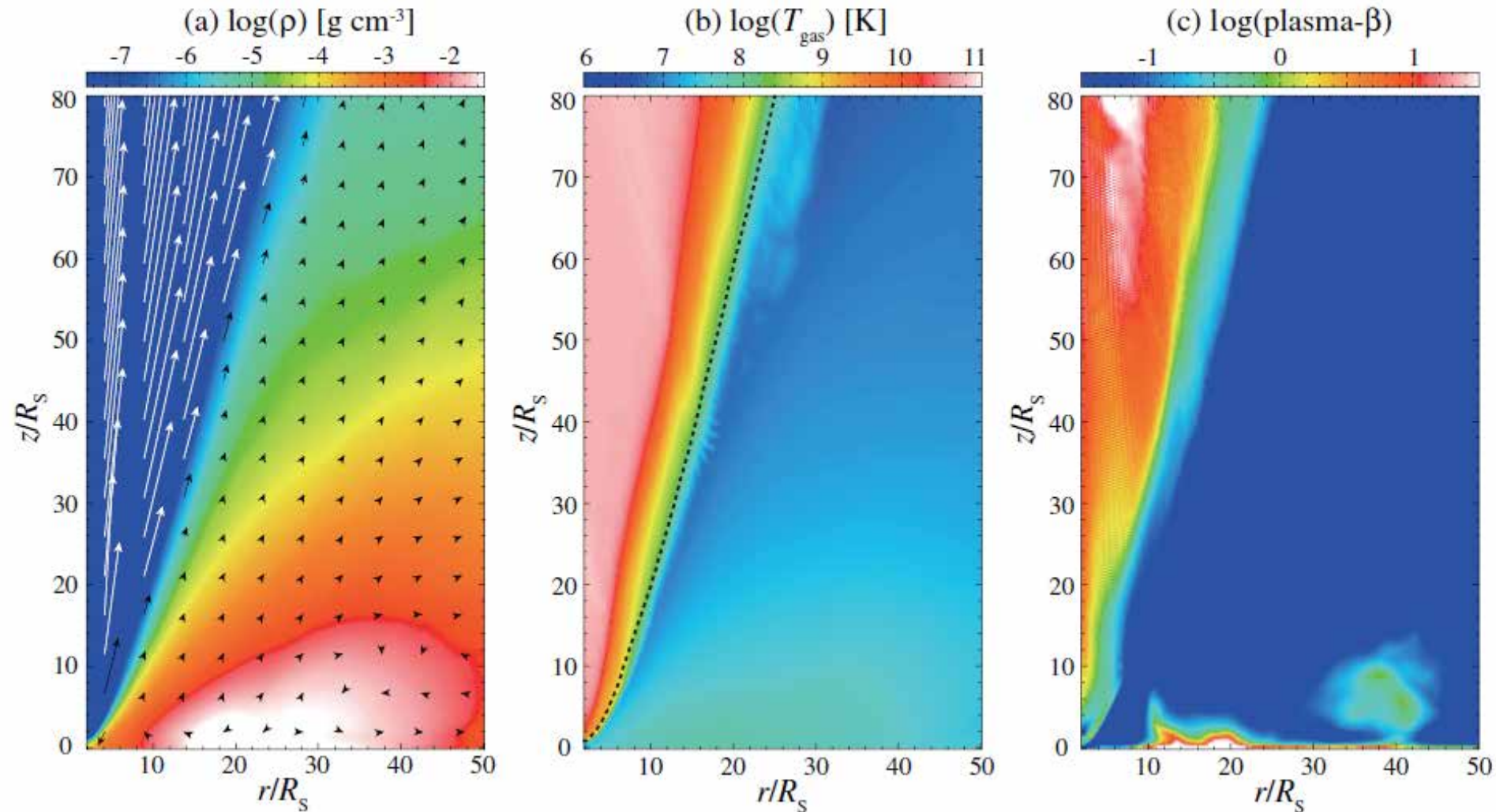


$$\text{Eddington ratio } n_E = 1.3$$

Super-Eddington Accretion & UFO (Ultra-Fast Outflow)

Ohsluga & Mineshige 2011, ApJ, 736, 2

2D Radiation Magneto-hydrodynamical simulation

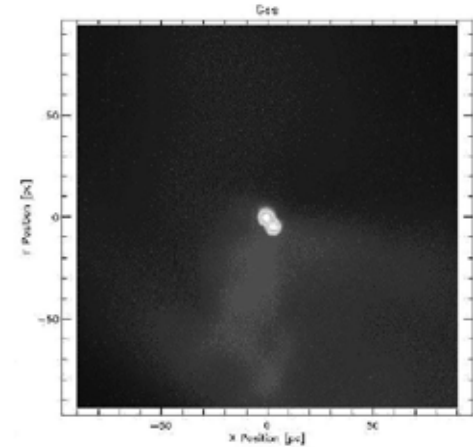


Direct Collapse to Massive Black Holes 超大質量星形成

Suppression of H₂ cooling by UV background

Bromm & Loeb 2003, ApJ, 596, 34

$5' 10^6 M_{\odot}$ MBH binary



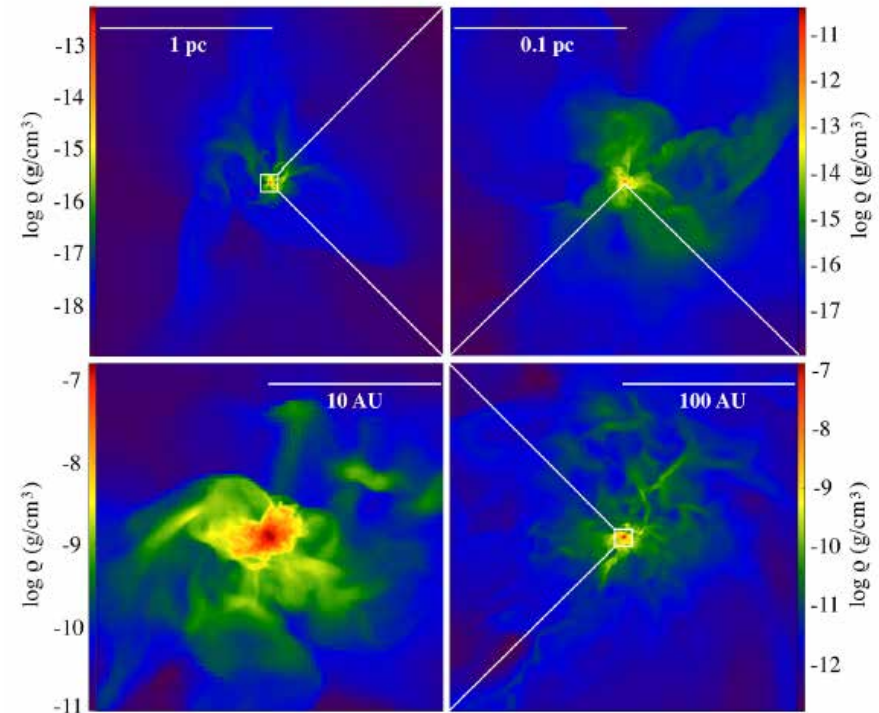
Cold Accretion Shock model

Inayoshi & Omukai 2012, MNRAS, 422, 2539

Warm cloud collapse model

Inayoshi, Omukai, Tasker 2014, MNRASL 445, L109

$>10^5 M_{\odot}$ MBH



GW150914 の7つの意義

重力波 (GW150914) 初検出!!!

Advanced LIGO, Sep 14, 2015, 09:50:45 UTC

(Abbott et al. 2016a, b, c, d, e, f, g, h, i)

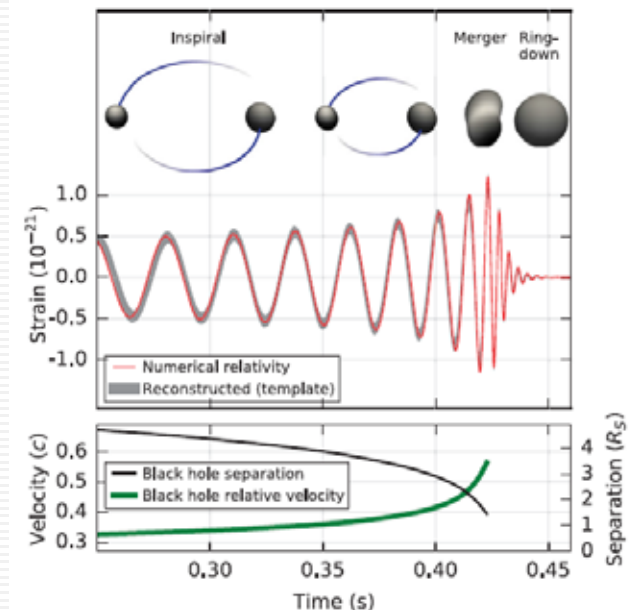
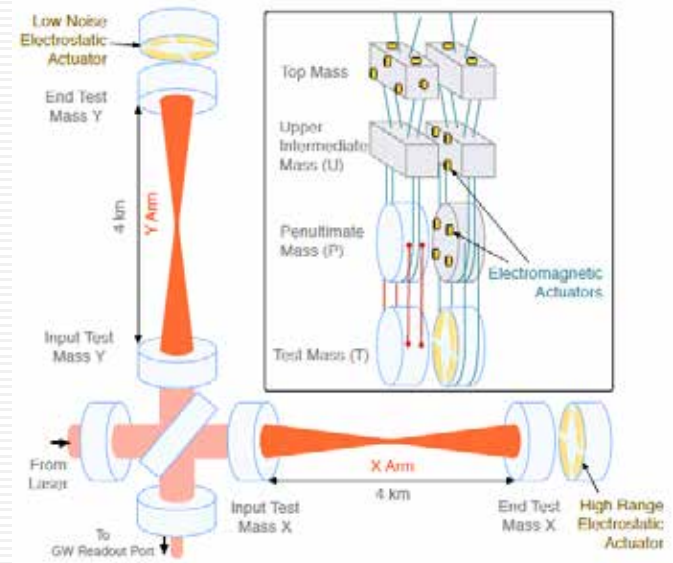
$36 M_{\odot}$, $29 M_{\odot}$ ブラックホールの合体 ($z = 0.09$)

Pop III の可能性

7つの意義

- 一般相対論の強い重力場の初検証
- ブラックホールの地平線の初確認
- 重い星質量ブラックホール ($\sim 30 M_{\odot}$) の初確認
- バイナリー・ブラックホールの初確認
- ブラックホール合体の初確認
- ブラックホール合体が重力波で起こることを初確認
- ブラックホール成長における合体の重要性

Quadruple suspension system



Mergers of $30 M_{\odot}$ Black Holes

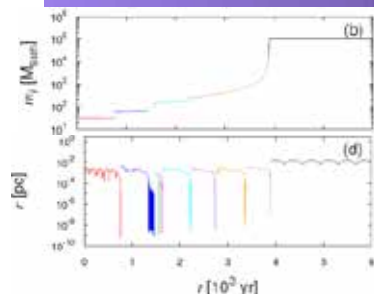
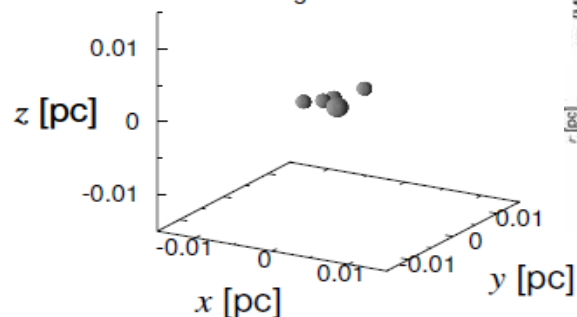
(Tagawa, Umemura, et al. 2015, MNRAS 451, 2174; 2016 arXiv:1602.08767)

Post-Newtonian N-body Simulations (2.5PN=GW)

Type A

Gas drag-driven merger

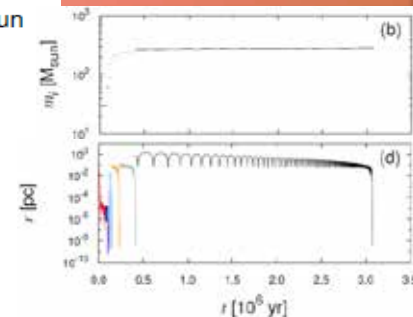
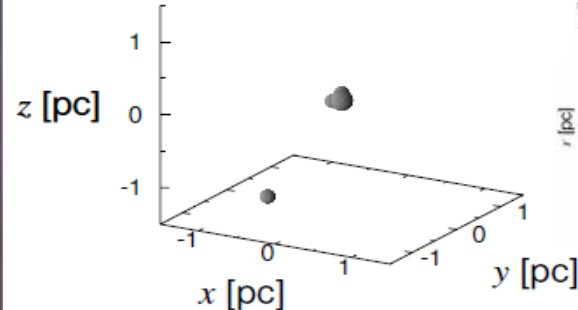
$t = 1.6 \times 10^3$ yr
 $m_{\text{ac,tot}} = 12 M_{\text{sun}}$
 $N_{\text{merge}} = 4$



Type B

Interplay-driven merger

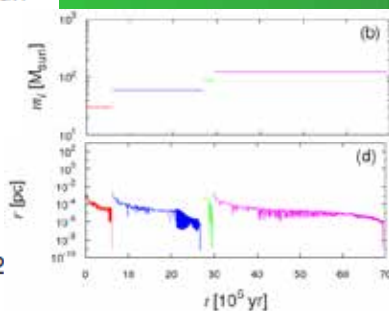
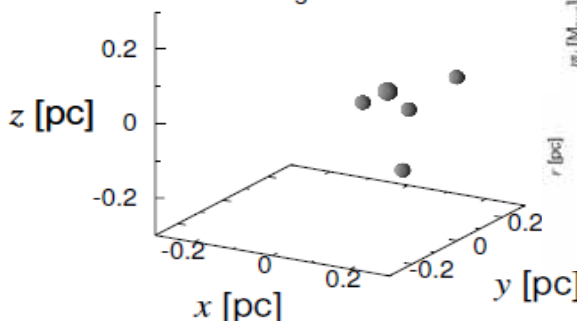
$t = 1.5 \times 10^5$ yr
 $m_{\text{ac,tot}} = 3.7 \times 10^{-2} M_{\text{sun}}$
 $N_{\text{merge}} = 6$



Type C

Three body-driven merger

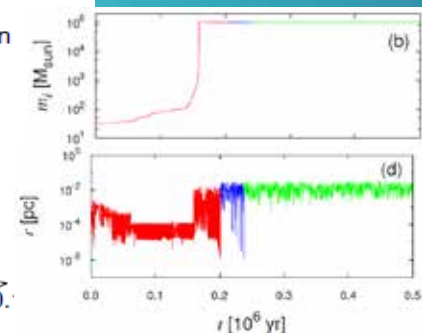
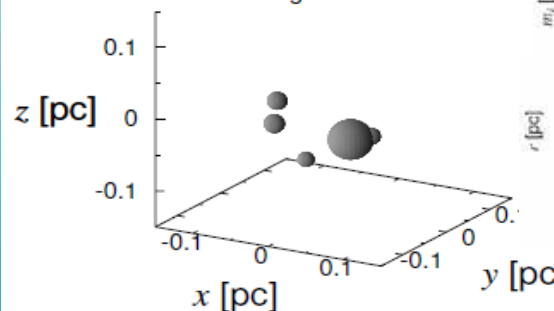
$t = 2.7 \times 10^7$ yr
 $m_{\text{ac,tot}} = 6.3 \times 10^{-3} M_{\text{sun}}$
 $N_{\text{merge}} = 2$



Type D

Accretion-driven merger

$t = 1.9 \times 10^5$ yr
 $m_{\text{ac,tot}} = 1 \times 10^5 M_{\text{sun}}$
 $N_{\text{merge}} = 0$



30 M_⊙ ブラックホールの合体 (Tagawa, Umemura, et al. 2015, 2016)

Post-Newtonian N体計算
2.5PN=GW

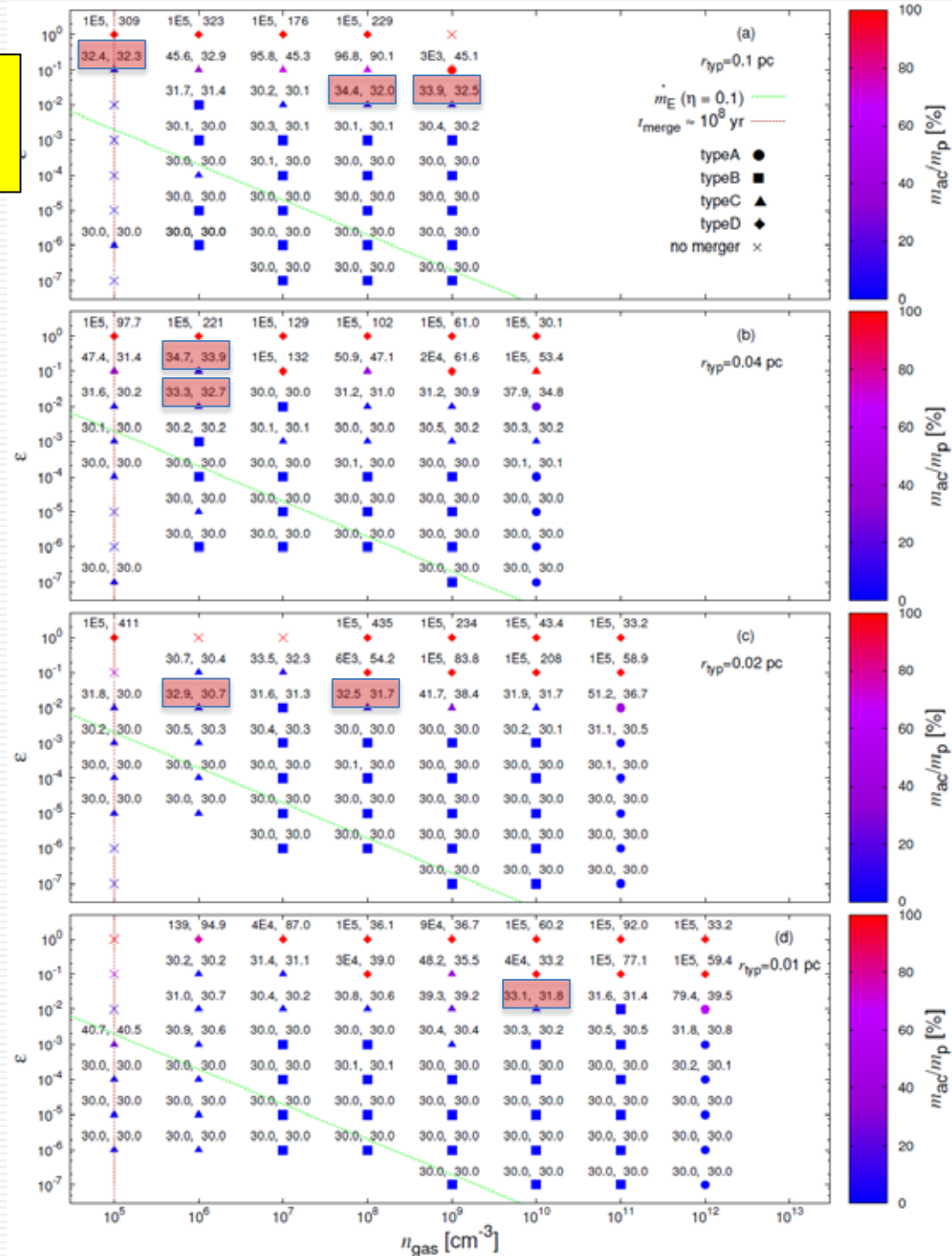
重力波 (GW150914) 検出

Advanced LIGO (Abbott et al. 2016)

$$m_1 = 36_{-4}^{+5} M_{\odot} \quad m_2 = 29_{-4}^{+4} M_{\odot}$$

GW150914のブラックホール質量に合うのは、全て3体相互作用による合体

降着質量は、数M_⊙の寄与がある

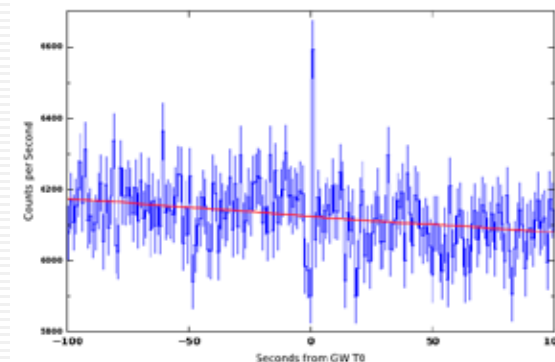
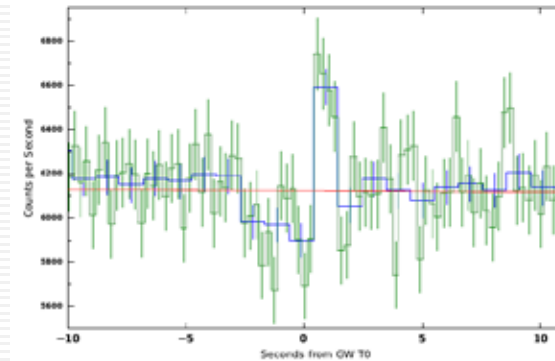
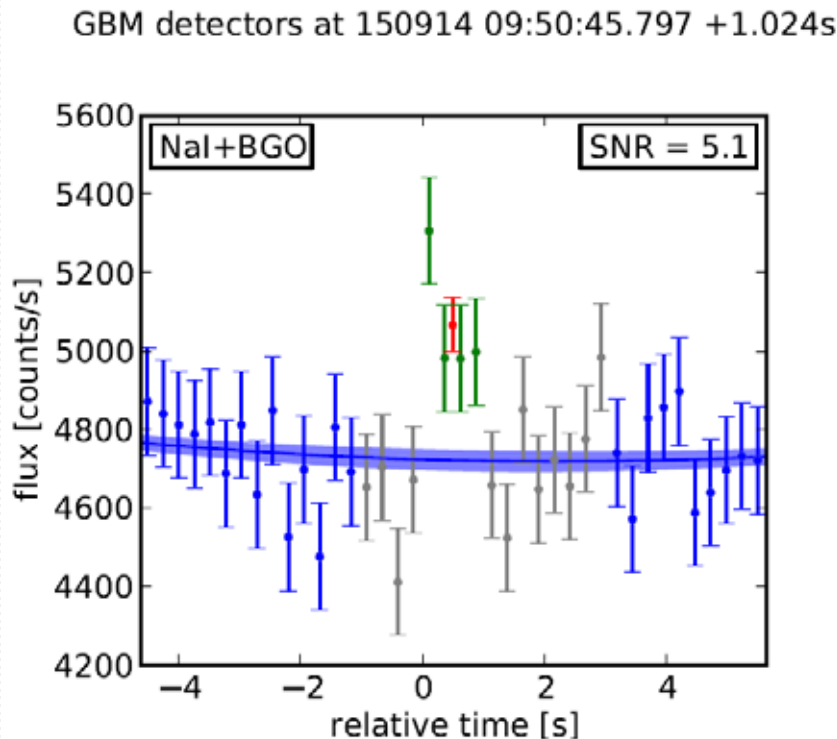


Counterpart in Hard X-Ray

Fermi GBM Observations of LIGO Gravitational Wave event GW150914

(Connaughton et al. 2016)

- ∅ GW150914 の0.4s後に >50 keV で weak transient source (a false alarm probability of 0.0022)
- ∅ Luminosity between 1 keV and 10 MeV = 1.8×10^{49} erg s⁻¹
- ∅ 方向ははっきり決まらないが, GW150914とは矛盾しない
- ∅ 他の astrophysical, solar, terrestrial, or magnetospheric activity とは相関せず。
- ∅ **weak short Gamma-Ray Burst を示唆**
- ∅ これまで, stellar mass black hole binary merger から予想されていたわけではない。



TAOへの期待 (SWIMS)

∅ First Stars

High-z GRB, SLSNeからIMFへの制限

∅ First Galaxies

初期進化史

Hell Ba a Emitter の観測

$z > 8$ 再電離期の銀河光度関数の決定

∅ First Massive BHs

初期成長過程の解明

(超臨界降着かBH合体成長か)